ISAS - INTERNATIONAL SCHOOL FOR ADVANCED STUDIES

Structural and vibrational properties of cesium hydride: a new high-pressure phase

Thesis submitted for the degree of

"Magister Philosophiæ"

CANDIDATE

Antonino Marco Saitta

SUPERVISOR

Prof. Stefano Baroni

October 1995

SISSA - SCUOLA INTERNAZIONALE SUPERIORE STUDI AVANZATI

TRIESTE
Strada Costiera 11

TRIESTE

SISSA ISAS
SCUOLA INTERNAZIONALE SUPERIORE DI STUDI AVANZATI
INTERNATIONAL SCHOOL FOR ADVANCED STUDIES

Structural and vibrational properties of cesium hydride: a new high-pressure phase

Thesis submitted for the degree of

"Magister Philosophiæ"

CANDIDATE

Antonino Marco Saitta

SUPERVISOR

Prof. Stefano Baroni

October 1995

Table of Contents

1 Introduction

The study of the properties of materials at very high pressures is a subject of great interest both from a theoretical and a technological point of view. The great development of the modern technology of ultrahigh pressures has given a considerable impulse to such studies. Nowadays, in a diamond anvil cell it is possible to produce hydrostatic pressures of the order of a few hundreds of GPa. This possibility is of great importance in geophysics, if we think that the typical pressures of the inner mantle of the earth are of this order of magnitude.

In solid state physics, this technology allows the exploration of regions of the phase diagrams falling in ranges of pressure once forbidden. This fact has led to the discover of new and unexpected structural phases of many materials, and so it is of current interest studying how such unknown phase transitions depend on the changes in the electronic structure induced by a strong external pressure.

In the last years a very large number of experimental and theoretical studies [1, 2, 3] have been carried out in order to investigate the phase diagram and the structural transitions of alkali halides. These compounds have a cubic lattice cell in their equilibrium structure,

but some of them show a spontaneous breaking of the high-symmetry phase when subject to a strong external pressure, with a transition to a low-symmetry structure. In particular, cesium iodide (CsI) has been found, both experimentally [4, 5] and theoretically [6, 7], to undergo a transition from the room pressure cubic-$B2$ (CsCl-like) structure to a new high-pressure orthorhombic phase.

A family of compounds quite similar to these salts is that of alkali hydrides. The alkali halides are fully ionic solids. The alkali hydrides, while being more covalent, are crystallographically analoguous to alkali halides and are expected to behave similarly with increasing pressure. At room pressure, the alkali hydrides have a cubic-$B1$ (NaCl-like) structure and, with the exception of LiH, have been observed to transform to the cubic-$B2$ structure at elevated pressures.

Very recently, an experimental work [8] on the structural properties of cesium hydride has shown a transition of this compound towards an orthorhombic lattice structure. The sample of CsH, put in a diamond anvil cell, was studied by means of energy dispersion x-ray diffraction (EDXD).

The authors find the $B1 \rightarrow B2$ transition to start at very low pressure (0.83 GPa). They fit their data for the latter structure to an equation of state in which the ratio between this cubic-$B2$ equilibrium volume V_{B_2} extrapolated to zero pressure and the cubic-$B1$ real equilibrium volume V_0 is $V_{B_2}/V_0 = 0.86$. The percentage volume change at the transition is about 8.4%. The transition from this $B2$ phase to the new orthorhombic is found to begin at 16.3 GPa with $V_{trans}/V_0 = 0.53$. The volume change of this second transition is observed

to be 6.3%. The experimentalists found in the EDXD spectra a good agreement between the intensities and the positions of the peaks of the CsH sample and the orthorhombic structure of CrB. Therefore, this phase was fitted to this structure, which falls in the *Cmcm* space group. Cesium hydride does not undergo any other structural transition up to 253 GPa, the highest pressure obtained in this experiment.

Gandehari *et al.* [9] studied also the behavior of the band gap of this material, finding that it remains an insulator up to the highest pressure investigated. They estimate, by extrapolation of their data, the gap closure to occur moreless at 1000 GPa. It is quite interesting to note that their results show that the system behaves as if it "does not want" to become metallic: the slope of the band gap *vs.* pressure is remarkably more negative in the cubic structure than in the orthorhombic high-pressure phase.

In the present thesis work, a theoretical study of the structural, vibrational and electronic properties of cesium hydride is presented in order to investigate this type of transitions so as to understand the driving mechanisms of the deformation of the cubic lattice that are involved in the transformation. These calculations are completely *ab initio*, and are based on the density functional theory (DFT) and density functional perturbation theory (DFPT).

In Chapter 2 the theoretical tools upon which this study is based are briefly described. In Chapter 3, we present our results on the structural and vibrational properties of cesium hydride. Chapter 4 is finally devoted to the conclusions.

2 Theoretical tools

The theoretical calculations of the structural. vibrational and electronic properties of cesium hydride presented in this thesis are completely *ab initio*, and are developed in the framework of density funcional theory. These calculations are performed at zero temperature, where the properties of interest can be obtained from the determination of the electronic ground state.

It is obviously impossible to solve exactly the many-body Schrödinger equations of electrons and nuclei in a crystal, but an approximation universally used in solid state physics. known as the Born-Oppenheimer approximation, allows to decouple the "fast" electronic variables from the "slow" ionic ones, by virtue of the great difference of masses. The system is thus divided in two subsytems: the electrons move in the potential of the fixed nuclei. following adiabatically their slow motion and remaining always close tho the quantum-mechanical ground state, while the ions are treated as they were classicle particles in the effective potential determined by the electronic ground state.

In the spirit of this approximation, it is possible to simplify the problem, and DFT provides the appropriate mathematical scheme for determining self-consistently the ground

state of the whole system.

2.1 Density functional theory

This theory was developed 30 years ago on the basis of the Hohenberg-Kohn theorem [10], which proofs the uniqueness of the external potential acting on the subsystem of the electrons as a functional of the electronic density $n(\mathbf{r})$. The energy of the electrons can be written as

$$E[n(\mathbf{r})] = F[n(\mathbf{r})] + \int V(\mathbf{r})n(\mathbf{r})d\mathbf{r}, \tag{2.1}$$

where $F[n]$ is a universal functional of the electronic density (independent on the external potential), and $V(\mathbf{r})$ is the "external" potential (with respect to the electrons) generated by the ionic cores.

In principle this problem should be solved via the constrained minimization of this functional, in general unknown, with respect to the electron B density, that must always be normalized to the number N of electrons:

$$\int n(\mathbf{r})d\mathbf{r} = N. \tag{2.2}$$

In order to apply this theory to actual calculations, Kohn and Sham proposed to separate the functional $F[n]$ into three distinct contributes:

$$F[n(\mathbf{r})] = T_0[n(\mathbf{r})] + \frac{1}{2}\int \frac{n(\mathbf{r})n(\mathbf{r}')}{|\mathbf{r}-\mathbf{r}'|}d\mathbf{r}d\mathbf{r}' + E_{xc}[n(\mathbf{r})]. \tag{2.3}$$

$T_0[n(\mathbf{r})]$ is the kinetic energy of a system of noninteracting electrons of density $n(\mathbf{r})$, the second is the classical Hartree term describing the Coulomb potential of the electrons,

while $E_{xc}[n(\mathbf{r})]$, defined by this formula, is known as the exchange and correlation energy and contains all the information about the many-body interactions among electrons that we do not know.

This way, the problem of constrained minimization becomes the problem of solving a set of self-consistent single particle equations:

$$\underbrace{\left[-\frac{\nabla^2}{2} + V_{SCF}(\mathbf{r})\right]}_{H_{KS}} \psi_i(\mathbf{r}) = \epsilon_i \psi_i(\mathbf{r}) \tag{2.4}$$

$$V_{SCF}(\mathbf{r}) = V(\mathbf{r}) + \int \frac{n(\mathbf{r}')}{|\mathbf{r} - \mathbf{r}'| d\mathbf{r}'} + v_{xc}[n(\mathbf{r})] \tag{2.5}$$

$$n(\mathbf{r}) = \sum_i |\psi_i(\mathbf{r})|^2 \theta(\epsilon_i - \epsilon_F). \tag{2.6}$$

These are the well known Kohn-Sham (KS) equations [11], where the Fermi energy ϵ_F is defined by the constraint on the number of electrons, $v_{xc}(\mathbf{r}) = \delta E_{xc}[n]/\delta n(\mathbf{r})$ is the exchange-correlation potential and the single particle orbitals satisfy the orthonormality constraint $\int \psi_i^*(\mathbf{r})\psi_j(\mathbf{r})d\mathbf{r} = \delta_{ij}$.

The Kohn-Sham equations are exact and still contain a completely unknown term in the exchange- correlation potential . In order to face this problem it is necessary, at this point, to introduce some approximations. A very natural approximation to DFT is the well-known local density approximation (LDA), in which the exchange-correlation energy is taken as a local *function* rather than a functional of the density:

$$E_{xc}[n(\mathbf{r})] = \int n(\mathbf{r})\epsilon_{xc}(n(\mathbf{r}))d\mathbf{r}, \tag{2.7}$$

and the potential is given by:

$$v_{xc}(\mathbf{r}) = \frac{d}{dn}(n(\mathbf{r})\epsilon_{xc}(n(\mathbf{r}))) = \mu_{xc}(n(\mathbf{r})). \tag{2.8}$$

In this approximation, the total energy of the crystal in its electronic ground state is:

$$\begin{aligned} E^{tot} &= -\sum_i \theta(\epsilon_i - \epsilon_F) \int \psi_i^*(\mathbf{r})\nabla^2\psi_i(\mathbf{r})d\mathbf{r} + \int V_{ion}n(\mathbf{r})d\mathbf{r} \\ &+ \frac{1}{2}\int \frac{n(\mathbf{r})n(\mathbf{r}')}{|\mathbf{r}-\mathbf{r}'|}d\mathbf{r}d\mathbf{r}' + \int n(\mathbf{r})\epsilon_{xc}(n(\mathbf{r}))d\mathbf{r} \\ &+ \sum_{\mathbf{R},s,s'}{}' \frac{Z_s Z_s'}{|\mathbf{R}+\tau_s-\tau_{s'}|}. \end{aligned} \tag{2.9}$$

LDA works surprisingly well for a large variety of systems, even more than any possible expectations, but it is known to be worse when describing weak atomic bondings. In the last decade, a lot of improvements to LDA were proposed [12, 13, 14, 15], but none of them seems to be a real "breakthrough" in this direction.

They are mostly based on the inclusion, in the dependence of the exchange and correlation functional, not only of the electronic density, but also of its gradient, and even of the Laplacian. For this reason it is commonly known as gradient-correction approximation (GCA). These kinds of new functionals are not satisfactory from a theoretical point of view, but certainly are able to describe better those situations in which LDA breaks down.

2.2 The plane-wave pseudopotential method

The actual solution of the KS equations can be obtained expanding the KS wavefunctions on a basis set. The most widely used choice of this basis is that of plane waves (PW), which

have the great advantage of being translationally invariant:

$$\psi_i(\mathbf{r}) = \psi_{n,\mathbf{k}}(\mathbf{r}) = \sum_{\mathbf{G}} \epsilon^{i(\mathbf{k}+\mathbf{G})\mathbf{r}} c_n(\mathbf{k}+\mathbf{G}). \tag{2.10}$$

where $\mathbf{k}$ belongs to the first Brillouin Zone (BZ) of the crystal. $\mathbf{G}$ is a reciprocal lattice vector and n is the band index. The PW basis set is infinite and it is usually truncated by choosing a kinetic energy cutoff through the condition:

$$|\mathbf{k}+\mathbf{G}|^2 \leq E_{cut}. \tag{2.11}$$

To treat explicitly all the electrons it would be necessary to choose a very large number of PW in order to describe accurately their rapid oscillations near the nucleus. This would request a very heavy computational effort for the calculation. It is possible to avoid this problem freezing the core electrons in the atomic configuration around the ions, and considering only the valence electrons.

To do this, one introduces the *pseudopotentials*, able to describe the interactions between these electrons and the *pseudoions* (ions+ core electrons). The valence electrons wavefunctions are considerably smoother near the nucleus, but are identical to the "true" wavefunctions outside the core region. This method is now well-established in computational physics, and the results are very accurate.

The widely-used norm-conserving pseudopotentials [16] consist of a local contribution for the radial function and a non-local one for the angular part:

$$v_s(\mathbf{r},\mathbf{r}') = v_s^{loc}(r)\delta(\mathbf{r}-\mathbf{r}') + \sum_{l=0}^{l_{max}} v_{s,l}(r)\delta(r-r')P_l(\hat{\mathbf{r}},\hat{\mathbf{r}}'), \tag{2.12}$$

where P_l is the projector on the angular momentum l.

This form of *semilocal* pseudopotential still is not the most convenient one from a computational point of view, and for this reason Kleinman and Bylander (KB) introduced [17] a fully non-local pseudopotential in which also the radial part of the potential is non-local:

$$v_s^{(NL)}(\mathbf{r},\mathbf{r}') = v_s^{loc}(r)\delta(\mathbf{r}-\mathbf{r}') + \sum_{l=0}^{l_{max}} v_{s,l}^{(NL)}(\mathbf{r},\mathbf{r}'), \tag{2.13}$$

where

$$v_{s,l}^{(NL)}(\mathbf{r},\mathbf{r}') = \sum_{m=-l}^{l} \frac{v_{s,l}(r)R_{s,l}(r)Y_l^m(\theta,\phi)Y_l^{*m}(\theta',\phi')R_{s,l}(r')v_{s,l}(r')}{\langle R_{s,l}|v_{s,l}|R_{s,l}\rangle}. \tag{2.14}$$

This form of the potential allows a very convenient simplification of its matrix elements in reciprocal space, where the KS equations are iteratively solved.

The only problem which one is often compelled to face (this is in fact our case) with the KB form of pseudopotentials is that of *"ghosts"*. The non-local character of the KB potential makes possible that eigenstates with nodes have lower eigenvalues than the zero-node state [18]. However there is a standard way of eliminating this problem, simply by collecting together in a different manner all the l-different contributes to the potential.

2.3 Lattice dynamics

In the conceptual scheme of density functional theory, it is also possible to study the vibrational properties of a crystal, treating ions as classical particles. In the harmonic approximation the total energy of the system can be expanded in a Taylor series in the atomic displacements $\mathbf{u}$:

$$E^{tot}[\mathbf{u}] = E_0^{tot} + \frac{1}{2}\sum_{\mathbf{R},s,\mathbf{R}',s'} \frac{\partial^2 E^{tot}}{\partial \mathbf{u}_s(\mathbf{R})\partial \mathbf{u}_{s'}(\mathbf{R}')}\mathbf{u}_s(\mathbf{R})\mathbf{u}_{s'}(\mathbf{R}') + \mathcal{O}(\mathbf{u}^3), \tag{2.15}$$

where $\mathbf{u}_s(\mathbf{R})$ is the displacement of the s-th atom in the unit cell in $\mathbf{R}$. The equations of motion of the ions are:

$$M_s \ddot{u}_{\alpha s}(\mathbf{R}) = - \sum_{\mathbf{R}',s',\beta} C_{\alpha s,\beta s'}(\mathbf{R}-\mathbf{R}') u_{\beta s'}(\mathbf{R}'), \tag{2.16}$$

where α and β are the polarizations of the modes, and $C_{\alpha s,\beta s'}(\mathbf{R}-\mathbf{R}')$ are the interatomic force contants which, thanks to the translational invariance of the crystal, depend just on $(\mathbf{R}-\mathbf{R}')$, rather than on $\mathbf{R}$ and $\mathbf{R}'$ separately.

The solution of those equations of motion can be written in Bloch form:

$$\mathbf{u}_s(\mathbf{R}) = \frac{1}{\sqrt{M_s}} \mathbf{u}_s(\mathbf{q}) e^{i(\mathbf{qR}-\omega t)}. \tag{2.17}$$

where the wave vector $\mathbf{q}$ belongs to the BZ. We obtain a linear system:

$$\omega^2 \mathbf{u}_s(\mathbf{q}) = - \sum_{s'} \mathbf{D}_{ss'}(\mathbf{q}) \mathbf{u}_{s'}(\mathbf{q}) \tag{2.18}$$

in which $\mathbf{D}_{ss'}(\mathbf{q})$ is called the *dynamical matrix* of the system and is simply proportional to the space Fourier transform of the interatomic force constants matrix $C_{\alpha s,\beta s'}$. From the diagonalization of this matrix one obtains the dispersion relations $\omega = \omega(\mathbf{q})$ of the system.

3 Results

In this chapter are presented and discussed all the theoretical calculations performed on cesium hydride, in order to describe its structural, vibrational and electronic properties, and to relate our results with those obtained by the experimentalists.

3.1 Technicalities

The first step of this work is the check on pseudopotentials. We have two possible choices for both the elements of the compound. For hydrogen one can use the bare $1/r$ potential, or a potential generated following the method proposed by von Barth and Car [19]. The potential is fitted to the analytical form:

$$v^{loc}(r) = \frac{-Z_v}{r} erf(r\sqrt{\alpha_c}). \quad v_l(r) = (a_l + b_l r^2) exp(-\alpha_l r^2). \tag{3.1}$$

For cesium we have a choice between two fully non-local pseudopotentials, one generated with the Kerker's procedure, and fitted to the same analytical form already shown, and the other, in numerical form, generated with the technique of Martins and Troullier [20]. Each of these potentials suffer the presence of a "ghost" state when put in the computationally more

convenient KB form, but they are eliminated simply writing in a different but equivalent manner the local part of the pseudopotential.

It is necessary to include, as valence electrons, also the $5s$ and $5p$ states, because pseudopotentials with the only inclusion of the $6s$ electron yield completely unrealistic results. However, cesium remains one of the elements more difficult to treat with pseudopotentials: it has the $4d$ electrons not so far in energy from those other which we consider explicitly. From the other side, it would be computationally too expensive to consider 19 valence electrons per atom.

The main part of our calculations is performed within LDA, with the electron-gas exchange-correlation energy and potential determined by Ceperley and Alder [21] as interpolated by Perdew and Zunger [22]. As we will see later, a part of the structural calculations is instead carried out using the so-called gradient corrections (GC), in order to yield more accurate results, comparable with experiments.In particular, we use the Becke exchange energy [13] and the Perdew correlation term [12].

In all calculations the sums over electronic eigenstates in the BZ are performed using some special points meshes in the Monkhorst and Pack scheme [23]. Plane waves up to a kinetic energy cutoff of 25 Ry are included in the basis set.

3.2 Energetics from First-Principles: LDA and beyond

The first step of a total-energy calculation is the test of convergence of the resulting energies with respect to the main numerical approximations, the cutoff and the finite sample mesh

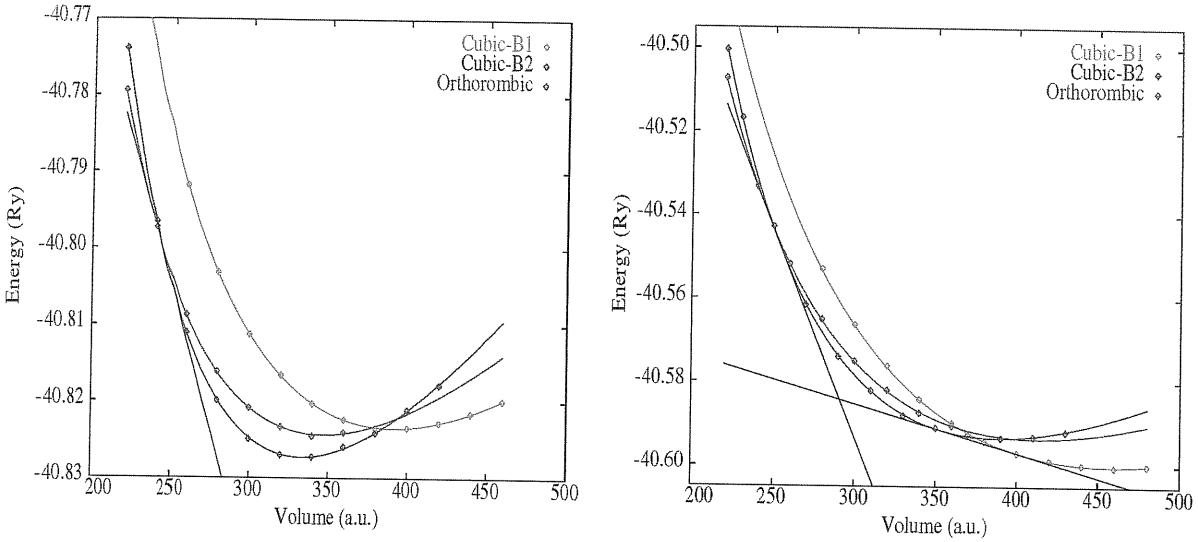

Figure 3.1: LDA and GC theoretical Murnaghan curves.

of k-points in reciprocal space.

The zero-pressure equilibrium structure of cesium hydride is the cubic-$B1$. We fit our results to a Murnaghan equation of state [24]:

$$P(V) = \frac{B_0}{B_0'}\left[\left(\frac{V}{V_0}\right)^{-B_0'} - 1\right]. \tag{3.2}$$

The plots of the Murnaghan curves are shown in Fig 3.1.

In Tab. 3.1 we report our results for some structural properties of CsH in the three phases studied here: $B1$, $B2$, and CrB. The LDA fails to account for the stability of the rocksalt structure at zero pressure (negative $B1 \rightarrow B2$ transition pressure), while GC calculations predicts the correct sequence of transitions. GC-DFT also considerably improves the agreement between calculated and observed equilibrium lattice parameters and bulk moduli.

The inclusion of Cs semi-core states in the valence manifold implies that the pseudopo-

	Experiments	LDA	GGC
$a_0(B1)$	12.07 a.u.	11.62 a.u.	12.25 a.u.
$B_0(B1)$	8.0 ± 0.7 GPa	11.3 GPa	10.3 GPa
$B_0'(B1)$	4.0	3.3	2.8
$a_0(B2)$	7.23 a.u.	6.94 a.u	7.30 a.u.
$B_0(B2)$	14.2 ± 1.0 GPa	18.6	14.0
$B_0'(B2)$	4.0 ± 0.2	4.2	3.71
$P^*(B1 \longrightarrow B2)$	0.83 GPa	-0.8 GPa	1.5 GPa
$\Delta V(B1 \longrightarrow B2)$	8.4%	18 %	12.5%
$\Delta V(B2 \longrightarrow Ortho)$	6.3%	4.5%	4.0%
$P^*(B2 \longrightarrow Ortho)$	17.5±1.5 GPa	11.0±0.5 GPa	14.6±1.0 GPa
V^*/V_0	0.53	0.63	0.54

tential transferability is optimal around the corresponding orbital energies, rather that the energies of the valence states. As a consequence this treatment of semi-core states—although essential to obtain sensible results— might require the use of more than one reference state in order to ensure optimum transferability. Whether or not the relatively poor quality of the LDA predictions is due to deficiencies in the Cs pseudopotential and the improvements achieved by using GC-DFT due to a fortuitous cancellation of errors is a matter which deserves further investigations. In any events, our results seem to confirm the importance of the gradient corrections to the LDA in the description of structural phase transitions, recently claimed in the case of diamond to β-tin transition in silicon [25].

Both LDA and GC-DFT calculations correctly predict that a transition from the $B2$ to the CrB phases would occur at pressures somewhat larger than 10 GPa. In this case

too, GC-DFT gives a value of the transition pressure in closer agreement with experiments (15 *vs.* 17 GPa). Note however that—due to hysteresis effects—an estimate done when loading the sample only provides an upper limit to the transition pressure. Also the volume discontinuity and the ratio between the transition volume and the equilibrium one are well reproduced by our calculations.

3.3 Distortion of the high-symmetry phase

The low-pressure transition $B1 \rightarrow B2$ is typical of ionic solids, and so it is not interesting to us.

After having predicted, both in LDA and in GC calculations, the high-pressure transition to the orthorhombic phase, we instead focus our attention on the possible mechanisms of distortion involved in this transition.

The CrB structure can be viewed as resulting from a continuous deformation of the cubic $B2$ structure in which a shear of the cubic edges in the (110) planes is coupled with a vibrational distortion of the atomic lattice, having the periodicity of a zone-border transverse phonon at the M point of the Brillouin zone (BZ). $\mathbf{q} = (\frac{1}{2}, \frac{1}{2}, 0)$, and polarized along (001). In Fig. 3.2 we display how the distorted (110) plane (Fig. 3.2c) results from the combination of the elastic (Fig. 3.2a) and the vibrational (Fig. 3.2b) deformations. In the ideal CrB structure the a and b crystallographic parameters indicated in Fig. 3.2 are in the ratio $b/a = 2\sqrt{2}$ which would be appropriate to a cubic structure. Due to the lower symmetry of the CrB structure with respect to the cubic one, the actual value of b/a

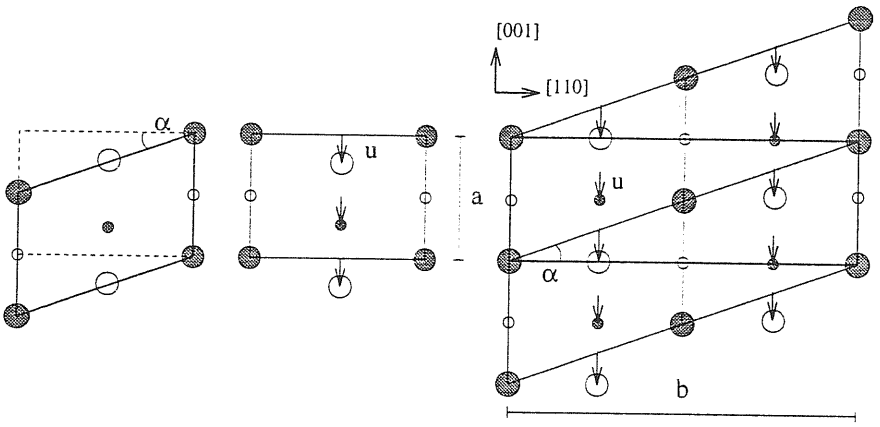

Figure 3.2: Decomposition of the distortion leading to the CrB structure (right panel) into an elastic (left panel) and a vibrational (middle panel) contributions. Large and small circles represent Cs and H atoms respectively. Dark and light shading refer to the topmost and second (110) layers respectively.

slightly differs from the ideal one and depends somewhat on pressure. This dependence is however very weak: at the transition pressure, for instance, one has $b/a \approx 2.9$. The third crystallographic axis is orthogonal to the ab plane, and the corresponding crystallographic parameter has an ideal value $c = \sqrt{2}a$. The pressure dependence of c/a is somewhat stronger than that of b/a: at the transition, for instance, one has $c/a \approx 1.3$.

In Fig. 3.3 we show the $T = 0$ enthalpy, $H = E + PV$, of the system constrained to a given elastic deformation, as a function of its amplitude, $t = \tan(\alpha) \times b/a$ [26]. We see that at any positive pressure a second minimum exists at $t = 1$, corresponding to the CrB orthorhombic structure. Actually, the exact value of $\tan(\alpha)$ slightly depends on pressure because so does b/a. For pressures higher than $P_2^* \approx 11$ GPa the second minimum becomes

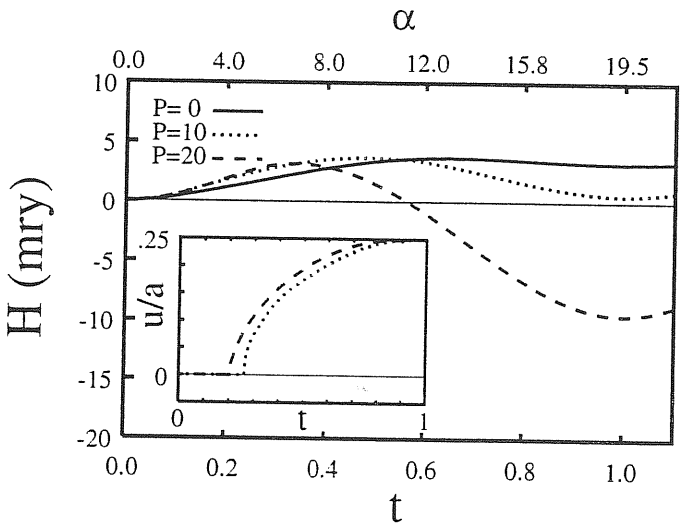

Figure 3.3: Enthalpy *vs.* angle of deformation for different fixed external pressures.

more stable giving rise to a first-order phase transition. The amplitude of the vibrational distortion, $u \equiv x/a$, which minimizes the enthalpy, u_{min}, depends on t, but for $t = 1$ it is constrained by symmetry to be $u_{min} = 1/4$. independent of pressure. The dependence of u_{min} upon the amplitude of the elastic distortion, t, is shown in the inset of Fig. 3.3. We see that u_{min} remains equal to zero up to a critical value of $t = t^{\star}$ which depends on pressure, and that it saturates to 1/4 for $t = 1$. This behavior is typical of the order parameter at a second-order phase transition, and it indicates therefore that a phonon frequency softens when the elastic distortion becomes larger than $t^{\star}$.

In Fig. 3.4 we display the M_2^- phonon frequency as a function of t at different pressures, P, (left panel) and as a function of P for different elastic distortions.

The softening of the M_2^- frequency in correspondence to some value of the elastic distortion could have been expected on the basis of symmetry considerations. To see this, let

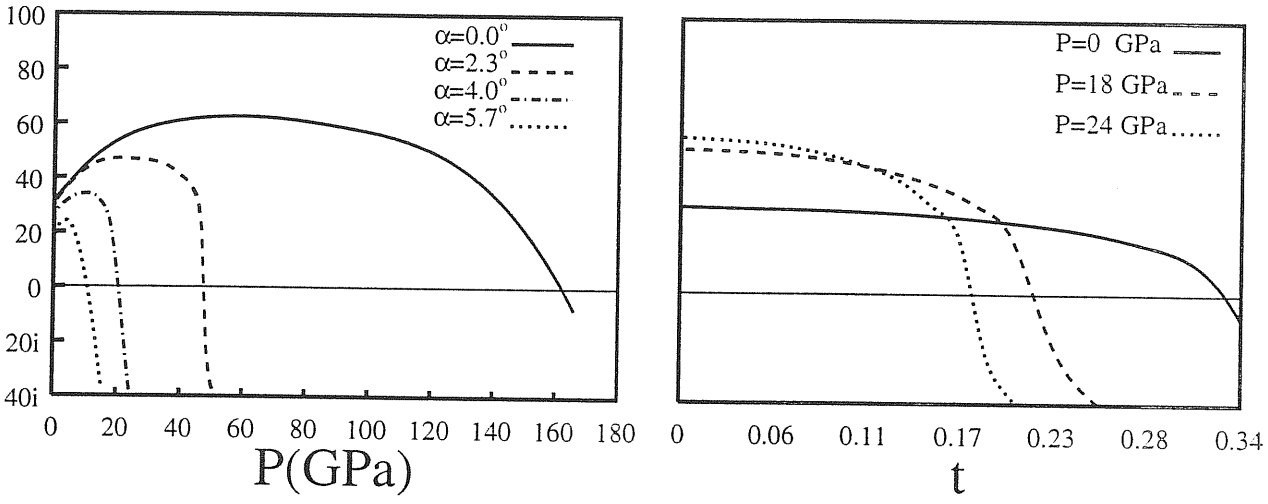

Figure 3.4: Phonon frequency as a function of external hydrostatic pressure for different angles of deformation (indicated in the figure) of the cubic structure.

us consider the crystal energy as a function of t and u, $E(t,u)$. Crystal symmetry requires that $E(t,u) = E(\pm t,u) = E(t,\pm u) = E(t+2,u+\frac{1}{2}) = E(t+2,u-\frac{1}{2})$. These relations imply that $E(t,u)$ is stationary at the point $(t,u) = (2,0)$. This point lies in between the four equivalent minima at $(0,0)$, $(2,\pm\frac{1}{2})$, and $(4,0)$. Assuming that the energy landscape is simple, we arrive at the conclusion that $(2,0)$ is a maximum. In particular, one has that $\partial^2 E/\partial u^2 < 0$, and hence there exists a value of $0 < t < 2$ for which $\omega^2_{M_2^-} \sim \partial^2 E/\partial u^2 = 0$. The orthorhombic phase corresponds to the $(1,\frac{1}{4})$ point in the (t,u) plane which is also stationary because of symmetry. This point is located halfway between the two points $(1,0)$ and $(1,\frac{1}{2})$ which are equivalent by symmetry and stationary with respect to variations of u $(\partial E/\partial u = 0)$.

If $t^\star$ were larger than 1, $\partial^2 E/\partial u^2$ would be positive at $(1,0)$ and $(1,\frac{1}{2})$, and therefore the

assumption of a simple energy landscape would imply that $(1, \frac{1}{4})$ is a maximum with respect to u, and the orthorhombic structure unstable. It is easy to see that a first-order transition with a discontinuous variation of u would occur in this case as the elastic distortion crosses $t = 1$. In fact, in this case the line $(t, 0)$ is stable with respect to variations of u. up to $t = 1$. For $t > 1$ one has that $E(t, \frac{1}{2}) < E(t, 0)$. Hence, a discontinous jump in u would occur at $t = 1$ where $E(t, \frac{1}{2}) = E(t, 0)$.

Arguments similar to those expounded above show that for $t^\star < 1$ the $(1, \frac{1}{4})$ point is a minimum in the u direction, while nothing can be concluded in principle for other directions. but the fact that local stability is allowed. Our calculations indicate that in the present case $t^\star < 1$ and that the CrB structure is indeed locally stable. For pressures higher than 11 GPa (15 GPa within GC), this structure is favored with respect to the cubic one, giving thus rise to a first-order transition.

3.4 Electronic structure *vs.* volume and symmetry

In the last part of the work developed in this thesis, we want to investigate the physical origins of the occurring phase transition $B2$—orthorhombic. First of all, there are geometrical reasons that make the orthorhombic structure closer-packed than the cubic one. In fact. if we focus our attention just on the cesium atoms sublattice. that is quite reasonable since a cesium atom is much larger than a hydrogen one, we can observe that in the $B2$ structure it has 6 other cesium atoms as nearest-neighbors. A simple analysis of the crystallography of the system shows instead that in the high-pressure phase. in a sphere of radius $1.1a_0$

centered on each cesium atom there are 8 other cesium atoms.

It seems however that another strong reason should be at the origin of this transition. We know in fact, from experimental results [9], that the energy gap between the valence and the conduction bands is strongly dependent on the symmetry of the system.

It has an experimental value of 4.4 eV at zero pressure, but it is shown to go down quite rapidly for an increasing external pressure, in the range of cubic-$B2$ stability. After having become orthorhombic, the system exhibits a quite slower closure of the energy gap, and it is still an insulator even at the highest applied pressures. This behavior suggests that the transition may occur just in order to balance the incoming metallization of the system.

To this aim, we determine the electronic structure of the system for different pressures and in the different phases. In fig. 3.5 we see such bands for an external pressure slightly higher than that of transition. We know that the calculation of the excited states is a purpose beyond density functional theory, which is a ground state theory. However, it is able to give results in general qualitatively and semiquantitatively correct, and so we can be confident that the correct trend is well predicted. In this limitations, we observe that the energy gap is smaller in the cubic phase than in the orthorhombic.

It is very interesting to look at what happens if we increase the external pressure up to 40 GPa: as we can see in fig. 3.6, if the system had the cubic structure, it would be metallic. On the other hand, in the orthorhombic structure, which is the most stable for these values of pressure, the system is still non-metallic. The fundamental band gap in the $B2$ phase corresponds to a transition from the X to the R point of the BZ. We note that

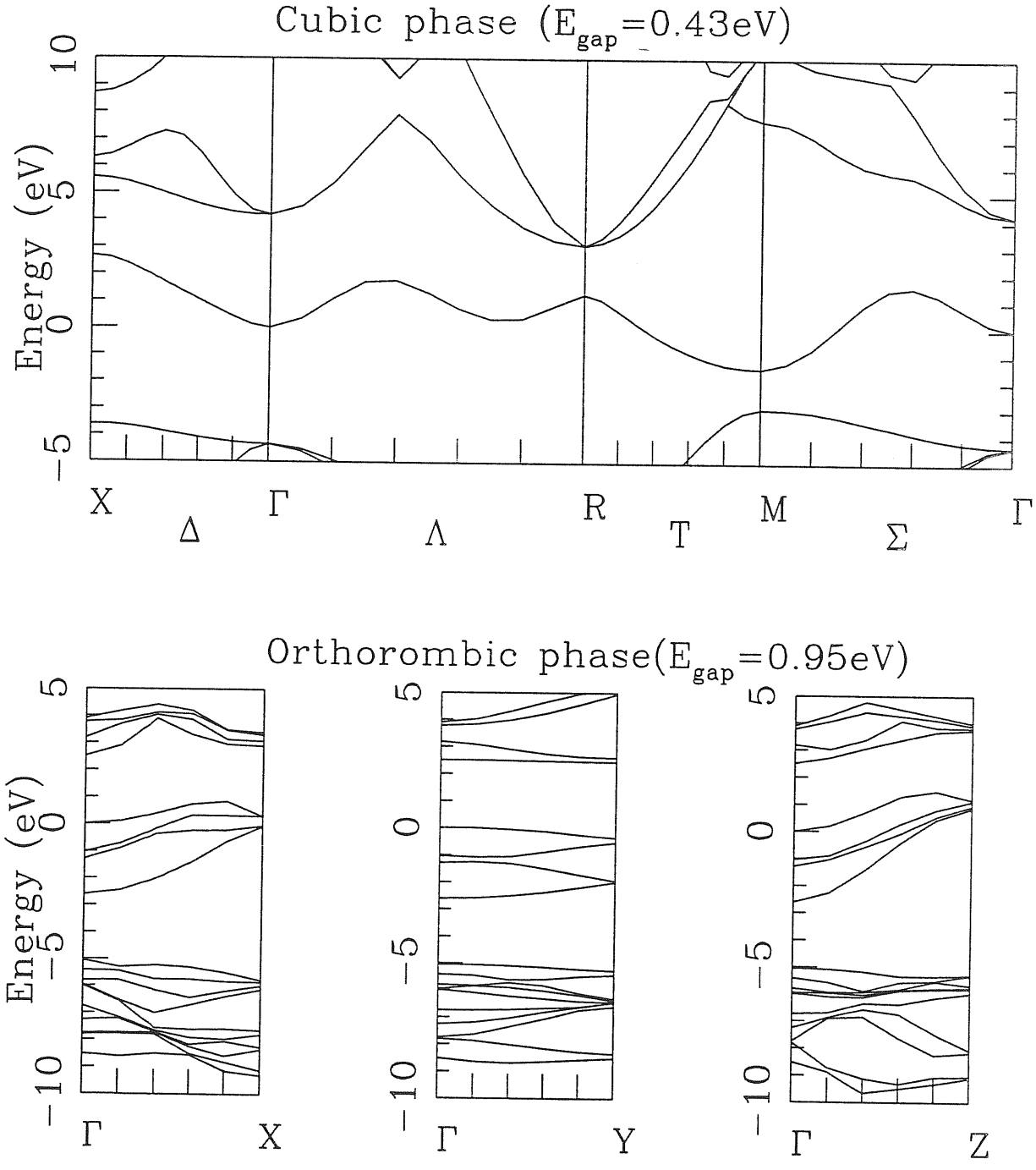

Figure 3.5: Electronic bands for both structures at 20 GPa

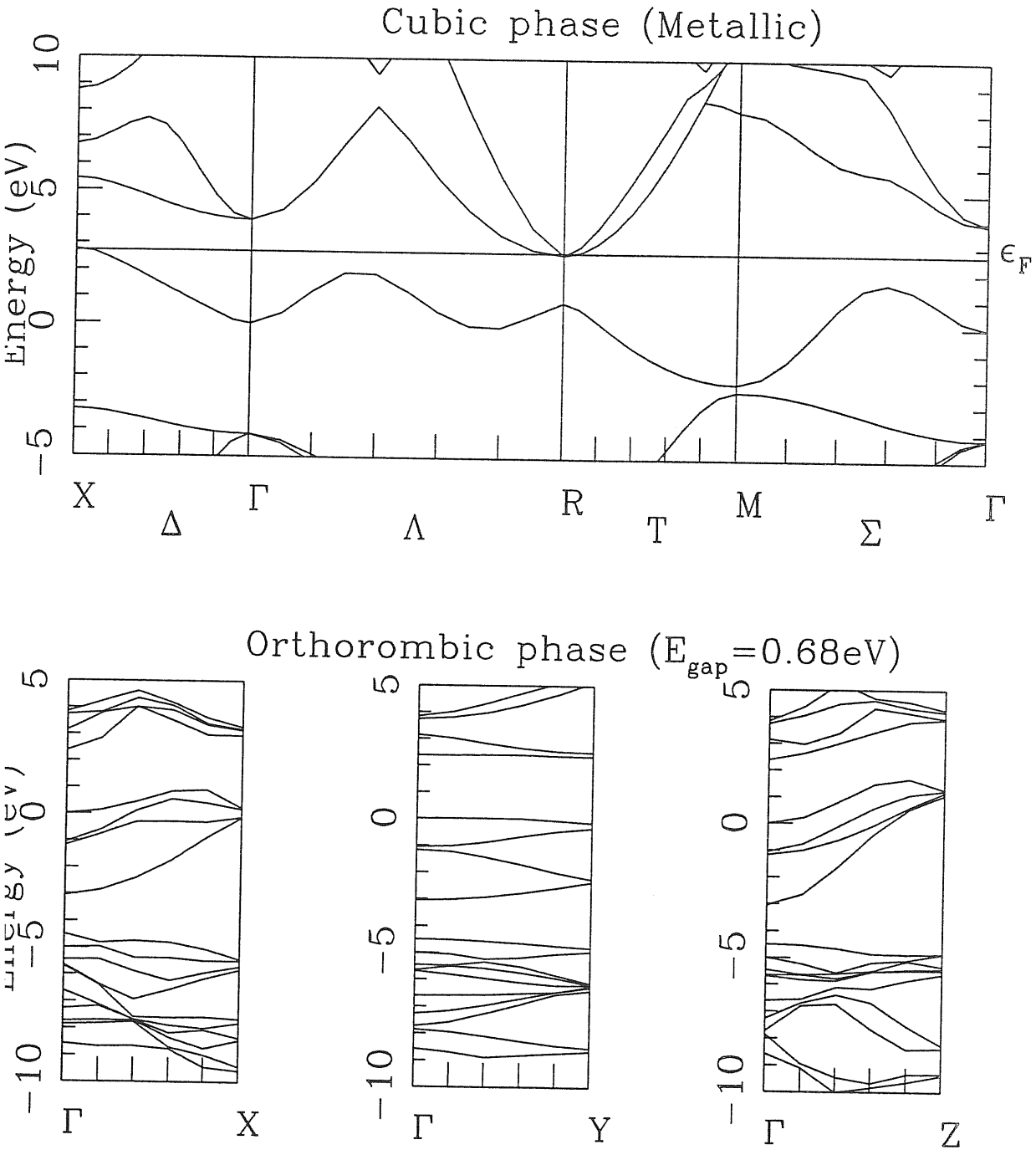

Figure 3.6: Electronic bands for both structures at 40 GPa

the wavevector which is the difference between these two corresponds to the M point of BZ. which should be the wavevector of the phonon involved in the elastic distortion.

In the distorted structure, the small value, for any pressure, of t^* found in our calculations can be also traced back to the electronic properties of this material, because the phonon softening is related to the metallization of the system under the elastic deformation described in the previous section. In fact we have found that the band gap, corresponding to the same transition between the $\mathbf{q}$-points equivalent to X and R of the BZ in the $B2$ phase, closes when increasing the amplitude of the deformation and vanishes for a value of t slightly smaller than t^*. When the amplitude of the elastic distortion is larger than t^*, the spontaneous vibrational distortion due to phonon softening re-opens the band gap and makes the orthorhombic phase insulating.

4 Conclusions

In this work we analyze the properties of cesium hydride at high pressure. We are able to predict the recently discovered orthorhombic phase transition with a good estimate of the transition pressure both in LDA and in GC. In fact we find a value of 11 and 15 GPa. respectively, while the experimentally found value of about 17 GPa is only an upper limit. because of hysteresis effects.

We investigate a reasonable mechanism of deformation of the cubic structure which involves an anisotropic elastic ("first-order") distortion coupled with a vibrational ("second-order") deformation of the crystal lattice. For each value of the external pressure there exists a critical strain that makes the structure unstable with respect to lattice vibrations. Small anisotropic stresses dramatically lower the phonon-softening pressure, which in the cubic phase would be of about 160 GPa.

This behavior is strictly related to the electronic band structure of this material, which would become metallic in the cubic phase. Both in the experiments and in our calculations. it is observed a gap closure with increasing pressure. In particular. we find that the fundamental band gap corresponds to a transition between the X and R points of the BZ of the

$B2$ structure, whose **q**-vector difference corresponds to the M point. It suggests that the system gains energy re-opening the band gap with a phonon-softening-induced deformation of the lattice when elastically distorted, and this vibration actually corresponds a phonon of the same wavevector in the cubic phase (the M_2^- phonon), in agreement with our qualitative band structure analysis.

Acknowledgements

First of all, I want to thank my supervisor, prof. Stefano Baroni, for having introduced me in this field of research. It is not so easy to meet him more than two or three times in a month, but he is so patient in explanations, and his explanations are *always* so clear, that these few times are widely sufficient to learn a lot. I want also to thank Dario Alfé, with whom I have shared "joys and sorrows" of this work.

A person deserving very special thanks is Claudia, who in these six months has always been by my side from the scientific, but especially from the human point of view.

I want to thank Stefano de Gironcoli, for never having locked his door. I think that he is very helpful for any student, not only those ones involved in electronic calculations. I wish also to thank Paolo Giannozzi, for his precious advices on pseudopotentials: he has always answered immediately to my e-mails, also having never seen me!!

It is for me a great pleasure to thank all that people who, even if not directly involved in this work, have contributed to create a very relaxed and enjoying environment in room 31 and in whole Sissa: Daniele & Claudio, my new "brothers" in Trieste, the two "Glorious" Alice & Barbara, Lorenzo "il Paggetto", "Charles", Franz (from Messina), Franz (from

Bolzano), Giovanni and many more.

Finally I don't want to forget all those people who, even if living 1400 Km far from me, are always close to me: my parents, my sister, my brother, my "real" granny Maria, and all those friends who have been always present in my life.

My final thanks are devoted to two persons who introduced me in the world of scientific research: prof. Paolo V. Giaquinta, who is for me a "scientific father", and dr. Franco Buda. They have always strongly encouraged me during this year, even if I'm not still working with them, and I am particularly grateful of that.

Bibliography

[1] S. Froyen and M.L. Cohen, J. Phys. C **19**. 2623 (1986).

[2] T.-L. Huang and A. Ruoff, Phys. Rev. B **29**. 1112 (1984).

[3] E. Knittle and R. Jeanloz, Science **223**. 53 (1984).

[4] H.K. Mao, Y. Wu, R.J. Hemley, L.C. Chen. J.F. Shu, L.W. Finger and D.E. Cox, Phys. Rev. Lett. **64**, 1749 (1990).

[5] I.V. Aleksandrov, A.F. Goncharov, I.N. Makarenko and S.M. Stisov, Phys. Rev. B **43**. 6194 (1991).

[6] S. Baroni and P. Giannozzi, Phys. Rev. B **35**, 765 (1987).

[7] M. Buongiorno Nardelli, S. Baroni and P. Giannozzi, Phys. Rev. Lett. **69**, 1069 (1992).

[8] K. Ghandehari, H. Luo, A.L. Ruoff, S.S. Trail and F.J. DiSalvo, Phys. Rev. Lett. **74**. 2264 (1995).

[9] K. Ghandehari, H. Luo, A.L. Ruoff, S.S. Trail and F.J. DiSalvo, Solid State Comm. **95**, 385 (1995).

[10] P. Hohenberg and W. Kohn, Phys. Rev. **136**, B864 (1964).

[11] W. Kohn and J.L. Sham, Phys. Rev. **140**, A1133 (1965).

[12] J.P. Perdew and Y. Wang, Phys. Rev. B **33**, 8800 (1986).

[13] A.D. Becke, Phys. Rev. A **38**, 3098 (1988).

[14] C. Lee, W. Yang and R.G. Parr, Phys. Rev. B **37**, 785 (1988).

[15] J.P. Perdew and Y. Wang (unpublished).

[16] G.B. Bachelet, D.R. Hamann and M. Schlüter, Phys. Rev. B **26**, 4199 (1982).

[17] L. Kleinman and D.M. Bylander, Phys. Rev. Lett. **48**, 1425 (1982).

[18] X. Gonze, P. Käckell and M. Scheffler, Phys. Rev. B **41**, 12264 (1990).

[19] von Barth and R. Car (unpublished).

[20] N. Troullier and J.L. Martins, Phys. Rev. B **43**, 1993 (1991).

[21] D.M. Ceperley and B.J. Alder, Phys. Rev. Lett.**45**, 566 (1980).

[22] J. Perdew and A. Zunger, Phys. Rev. B **23**, 5048 (1981).

[23] H.J. Monkhorst and J.P. Pack, Phys. Rev. B **13**, 5188 (1976).

[24] F.D. Murnaghan, *Deformation of an elastic solid*, chap.4, John Wiley, NY, (1951).

[25] N. Moll, M. Bockstedte and M. Scheffler, Phys. Rev. B **52**, 2550 (1995).

[26] The analysis which follows is based on calculations performed within the LDA. Our conclusions, of course, do not depend on the form of the exchange-correlation functionals.